Hs-27, a Novel Hsp90 Inhibitor, Exhibits Diagnostic and Therapeutic Potential in Triple Negative Breast Cancer

Stella Belonwu

Under the supervision of Dr. Nimmi Ramanujam,
Department of Biomedical Engineering, Duke University

May, 2016

_____

Research Supervisor

_____

Faculty Reader

_____

Director of Undergraduate Studies

Honors thesis submitted in partial fulfillment of the requirements for graduation with Distinction in Biology in Trinity College of Duke University

Hs-27, a Novel Hsp90 Inhibitor, Exhibits Diagnostic and Therapeutic Potential in Triple Negative Breast Cancer

Abstract

Heat-shock protein 90 (Hsp90) is a molecular chaperone that is ubiquitously expressed in all cell types and essential for maintaining cell homeostasis by assisting in protein folding, de-aggregation, and degradation. Hsp90 is upregulated in all breast tumors, where it is present on the cell surface, unlike in normal cells, and supports signal transduction pathways important for tumor progression. Hence, Hsp90 has emerged as an attractive anti-cancer target. Triple negative breast cancer (TNBC) is a highly aggressive and difficult to treat subtype of breast cancer. Because TNBC is unresponsive to hormone therapies, there are no good therapy options available. Thus, Hsp90 may serve as a reasonable target for TNBC. Hs-27 is a novel Hsp90 inhibitor made by Dr. Timothy Haystead of Duke University's Department of Pharmacology and Cancer Biology. It was developed with a fluorescein contrast agent, which makes it suitable for diagnostics. Preliminary experiments with Hs-27 with breast cancer cell lines of different receptor subtypes show that it binds to ectopically expressed Hsp90 in tumor cells. *In vitro* therapy experiments also show that Hs-27 down-regulates client proteins implicated in tumor growth. In this study, I further establish Hs-27's diagnostic and therapeutic ability *in vivo* through hyperspectral and fluorescence imaging in dorsal skinfold window chamber tumor models in mice. Largely, I observed that at lower doses, Hs-27 allows for real-time, non-invasive imaging for cancer detection and at higher doses has the potential for therapeutic benefits.

Keywords: Hsp90; Breast cancer; Fluorescent Imaging

Abbreviations: TNBC; Triple-negative breast cancer; HER2+: Human epidermal growth factor receptor 2 positive; FITC; Fluorescein isothiocyanate

Introduction

Breast cancer is one of the three most commonly diagnosed cancers in women, accounting for 29% of all new cancers (Siegel et al., 2015). It is the leading cause of cancer death among women of ages 20 to 59 (Siegel et al., 2015). Typically diagnosed using mammography screening and corresponding biopsies, breast cancer treatments include surgeries, radiotherapy and use of chemotherapeutic agents. Unfortunately, these treatments have had limited success as a result of resistance and metastasis (Clarke et al., 2015), and there remains a need for additional diagnostic and treatment strategies.

Triple Negative Breast Cancer

Breast cancer subtypes are distinguished based on factors such as the presence of hormone receptors, which can help in choosing a treatment paradigm. Triple negative breast cancer (TNBC) is differentiated by tumors that do not express estrogen receptors (ER), progesterone receptors (PR), or human epidermal growth receptor 2 (HER-2) genes (Hudis & Gianni, 2011). TNBC is an aggressive form of breast cancer that poses a significant clinical challenge because it is unresponsive to hormone therapy, a common therapy used to treat most forms of cancers, which possess hormone receptors (Hudis & Gianni, 2011). Although TNBC is similar to other breast cancer subtypes through its capacity to spread, it is different in its association with a shorter median time to relapse and death, thus increasing the need to find better therapeutic strategies for this form of breast cancer (Hudis & Gianni, 2011).

Hsp90 as a possible anti-cancer target

Hsp90 is an abundant chaperone protein that was first discovered to stabilize proteins against heat stress. As a chaperone, its roles include maintaining cell homeostasis

through its assistance with protein folding, regulation of protein de-aggregation, and degradation pathways (Pearl & Prodromou, 2006; Wiech et al., 1992). Hsp90 is localized to the cytosol and present in the nucleus of cells, and has an N-terminal ATP binding domain, which is necessary for its function (Sawarkar et al., 2012). Hsp90 works through conformational changes as a result of ATP hydrolysis, and is regulated through its interactions with co-chaperones and by transcription factors (Mollapour & Neckers, 2012; Pearl & Prodromou, 2006; Trinklein et al., 2004).

Hsp90 is overexpressed two-to three fold in tumor cells in comparison to normal cells (Moulick et al., 2011; Sahu et al., 2012; Workman et al., 2007; Zagouri et al., 2010). Hsp90 upregulation might be a result of the tumor microenvironment where stresses such as heat, hypoxia and nutrient deprivation are common (Whitesell & Lindquist, 2005). Hsp90 is thought to stabilize approximately 400 client proteins, including Raf-1 kinase and Akt, which are known to contribute to apoptotic evasion and metastasis in cancer (Barrott et al., 2013; Callans et al., 1995; Nicholson & Anderson, 2002; Prince & Neckers, 2011; Samant et al., 2012). Upregulation of Hsp90 might thus serve to promote tumor cell proliferation and metastasis in the harsh tumor environments.

Interestingly, Hsp90 has a dichotomous interaction with the immune system. Its immunostimulatory effects include antigen presentation through the provision of danger/damage associated molecular patterns (DAMPs) to the innate and adaptive immune cell (Graner, 2015). On the other hand, it can interact with an important modulator of immune response such as matrix metalloproteinase-2(MMP2) to drive angiogenesis and further support the tumor microenvironment, a process which overrides the immunostimulatory role of Hsp90 (Graner, 2015; Parks et al., 2004). In sum, Hsp90's

tumor promoting effects both in modulating tumor progression and the tumor microenvironment may make it a good candidate to target in cancer therapy.

In addition to its potential role in promoting tumor progression, Hsp90 is also present on the surface of cells in all breast tumors and in the extracellular space, which correlates with a potential to metastasize (Becker et al., 2004; Sidera & Patsavoudi, 2008). Hsp90 upregulation in cancer cells thus could serve as an early indicator of malignant behavior (Cheng et al., 2012; Pick et al., 2007).

Hsp90's modulation of cancer cell metabolism

Breast cancer cells, like all cancer cells, consume increased amounts of glucose. These cells alter their metabolic pathways to increase energy to bolster proliferation in the body through processes such as DNA replication (Annibaldi & Widmann, 2010). Specifically, cancer cells prefer using glucose for aerobic glycolysis over oxidative phosphorylation pathways even in aerobic conditions, a phenomenon otherwise termed the Warburg effect (Annibaldi & Widmann, 2010; Dang, 2012). As a molecular chaperone, Hsp90 supports the maturation of a number of oncoproteins, some of which are implicated in cellular proliferation and metabolism (Trepel et al., 2010). One of such oncoproteins is Akt (also referred to as protein kinase (PKB)), an Hsp90 client protein which is upregulated in cancer and involved in glycolytic regulation through abnormal activation in the phosphatidylinositol 3-kinase (PI3K)/Akt/mammalian target of rapamycin(mTOR) pathway (Garcia-Echeverria and Sellers, 2008; LoPiccolo et al., 2008; Nicholson, & Anderson, 2002). The PI3K/Akt/mTOR pathway is an attractive therapeutic target as it is activated in many cancers and is thought to help with tumor maintenance and survival (Garcia-Echeverria and Sellers, 2008; LoPiccolo et al., 2008).

Since thwarting aerobic glycolysis represents a strategy to selectively target cancer cells, drugs such as BEZ-235 were developed as an anti-cancer target. BEZ-235 or NVP-BEZ235 (Novartis) is a dual PI3K/ mTOR inhibitor which exhibits significant antitumor activity (Roberts et al., 2012). It accomplishes inhibition of kinase activity in a broad panel cell lines by binding to the ATP-binding cleft of these enzymes (Garcia-Echeverria and Sellers, 2008). Overall, with the involvement of Hsp90 client proteins in metabolic regulation, there exists a potential to use Hsp90 as a target in cancer metabolism to achieve results comparable to those of BEZ-235 (Novartis).

Hsp90 inhibitors in progress

Hsp90 is an attractive target for the treatment of cancer because its inhibition results in simultaneous interruption of many signal transduction pathways that are important to tumor progression and survival (Moser et al., 2009). Hsp90 inhibitors have been studied for their anti-tumor activity for over 20 years, and as of 2013 have about 17 distinct drug formulations in clinical trials (Barrott & Haystead, 2013). Although Hsp90 is expressed in both cancer and normal cells, these Hsp90 inhibitors are selective for tumor cells over normal cells, with the exception of the retina (Chiosis & Neckers, 2006; Zhou et al., 2012). The inhibitors in practice take advantage of the increased selectivity for tumor cells, which unlike normal cells express Hsp90 on their surface that inhibitors directly bind to. Thus, this unique surface expression contributes to the high affinity of drug binding to Hsp90 (Barrott & Haystead, 2013).

Geldanamycin, a first generation Hsp90 inhibitor, is a natural antibiotic which was discovered to have antitumor effects through inhibiting the ATPase activity of the molecular chaperone Hsp90 (Miyata, 2005). Its discovery led to more research into the use

of Hsp90 inhibitors as chemotherapeutics for cancer (Barrott & Haystead, 2013). More recently, Geldanamycin has been modified to have lower toxicity and has been examined in phase I clinical trials (Miyata, 2005). To date, however, no Hsp90 inhibitors, have been approved for safety and efficacy reasons (Proia & Bates, 2014; Soga et al., 2013). Thus, there is a need to examine new Hsp90 inhibitors that have increased efficacy and minimal off-target effects. One promising second generation inhibitor, is Ganetespib, which interferes with multiple oncogenic pathways to reduce cell viability and has significantly fewer side effects in the cardiovascular system and liver (Proia & Bates, 2014; Proia et al., 2014; Ying et al., 2012).

Hs-27 and Specific Aims

Recently, Barrott and colleagues (2013) designed novel Hsp90 inhibitors that carry optical probes via a polyethylene glycol tether. Hs-27(See Appendix A) is one version of these synthesized tethered inhibitors that contains a derivative the fluorophore fluorescein isothiocyanate (FITC). The use of these probes is potentially powerful because they introduce real-time non-invasive imaging for cancer detection, unlike mammography, ultrasounds, and MRIs that lack the specificity to differentiate tumors from normal tissue (Esserman et al., 2009). Thus, Hs-27 could have potential as a theranostic, a diagnostic tool that can provide information about the malignant status of cells while working effectively to reduce their proliferation.

Initial investigation of Hs-27 showed that it promotes apoptosis of cancer cells and binds to ectopically expressed Hsp90, on the surface of breast cancer cells of different receptor subtypes*. In vitro* therapy experiments have also shown a decrease in tumor associated Hsp90 client proteins such as Raf-1 kinase and Akt. In this study, with the

expectation that Hs-27 will have promising outcomes in animal models, I continued investigation of Hs-27 to establish its ability to serve as a diagnostic and therapeutic tool through *in vivo* experiments with female nude mice. I conducted hyperspectral and fluorescence imaging on dorsal skinfold window chamber models (Figure 1) inoculated with a TNBC cell line to monitor drug delivery and uptake, and to observe the specificity of Hs-27. Overall, in addition to outcomes from the *in vitro* studies, my work has found that Hs-27 localizes more strongly in tumors compared to normal tissues. In total, my studies support the view that Hs-27 is a promising compound, which at low doses, helps with detection of malignant breast cancer cells through optical imaging and, at higher doses, may have therapeutic potential.

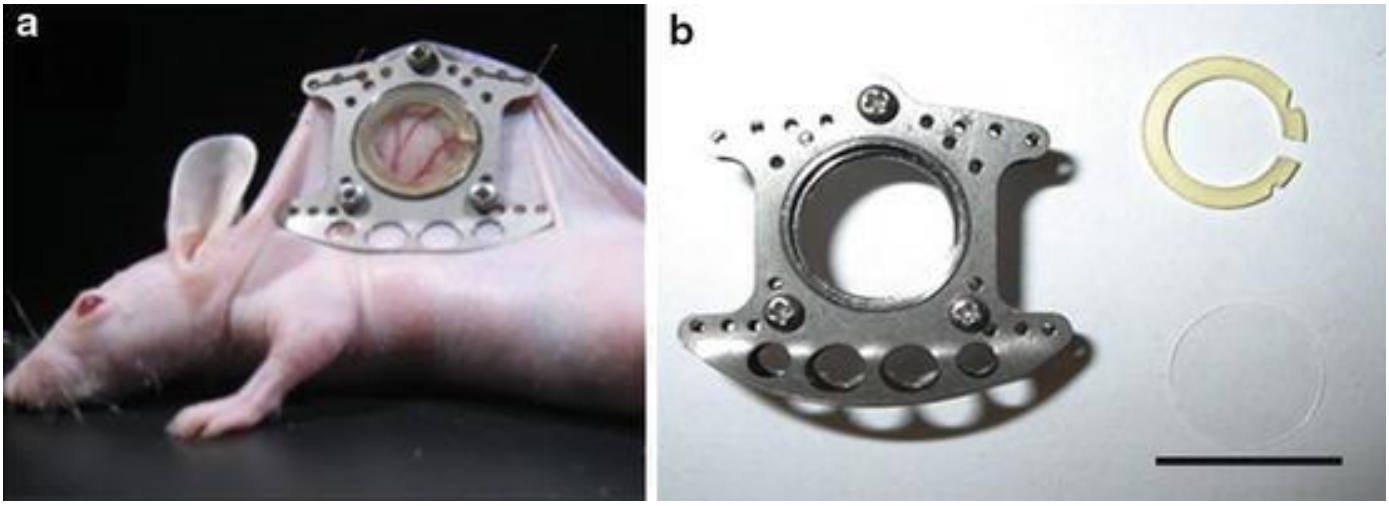

Figure 1. Illustration of the dorsal skinfold window chamber model. (A) Nude mouse with implanted dorsal skinfold window chamber. (B) Titanium window chamber, stopper and cover glass. Adapted from " Optical Coherence Tomography: Principles and Applications of Microvascular Imaging," by B.A Standish, A. Mariampillai, M.K.K. Leung, A. Vitkin, 2013, *Handbook of Coherent-Domain Optical Methods,* p.945-975. Copyright [2013] by Springer Science+Business Media New York. Adapted with permission.

Materials and Methods

Cell lines and Culture Conditions

Human triple negative breast cancer (TNBC) cell line MDA-MB-231, human epidermal growth factor 2 positive (HER2+) cell line BT-474, and estrogen receptor positive (ER+) and progesterone receptor positive (PR+) cell line MCF-7 were used in this study. Once obtained from the cell culture facility at Duke University, the cells were cultured according to different formulation guidelines. MDA-MB-231 cells were grown in Minimal Essential Medium Eagle (MEME, Sigma-Aldrich M4655) supplemented with 1% nonessential amino acids (NEAA, Gibco 11140), 10% Fetal Bovine Serum (FBS, Sigma-Aldrich F2442), 1% penicillin streptomycin (Sigma-Aldrich P4333) and 1% sodium pyruvate (Gibco 11360-070). BT-474 cells were grown in Roswell Park Memorial Institute (RPMI) 1640 Medium (Sigma R8758) supplemented with 0.56% Glucose, 45% (Sigma G8769), 1% HEPES (Gibco-Thermo 15630), 10% FBS (Sigma-Aldrich F2442), 1% penicillin streptomycin (Sigma-Aldrich P4333), 1% sodium pyruvate (Gibco 11360-070) and 0.25% Insulin (Gibco 12585-014). MCF-7 on the other hand was cultured in MEME (Sigma-Aldrich M4655) supplemented with 1% NEAA (Gibco 11140), 10% FBS (Sigma-Aldrich F2442), 1% penicillin streptomycin (Sigma-Aldrich P4333), 1% sodium pyruvate (Gibco 11360-070), and 0.25% Insulin (Gibco 12585-014). The cells were passaged every 2-3 days as needed and incubated at 37.0°C and 5.0% CO_2.

Cell plating and Confocal Imaging

Cells were cultured as described above. After 2-3 passages, approximately 500,000 cells of each cell line was plated in two 60 by 15mm tissue culture dishes (Falcon 353002).

One serving as the control and the other as the experiment. After 24 hours of incubation at 37 °C, 100uM of Hs27 was added in the experiment plate and 100uM DMSO in the control plate. After a 15 minute incubation at 37 °C, plates were washed three times with Phosphate-buffered saline (PBS; Corning 21-040-CV) to remove any unbound Hs-27, media was replenished, and Hoechst 33342 (Thermo Scientific 62249) as added to stain nuclear DNA. Cells were then imaged live with the Zeiss 780 upright confocal microscope.

In vivo window chamber study with MDA-MB-231 tumor cells

All animal work was performed according to guidelines provided by the National Institutes of Health and approved by the Duke University Institutional Animal Care and Use Committee. Female athymic nude mice (nu/nu, Duke Cancer Center Isolation Facility, Durham, NC) weighing between 20-30g were used for all *in vivo* studies. Animals were housed at the Duke University Vivarium with continual access to food and water under normal 12-hour light/dark cycles. The fluorescently labeled Hsp90 inhibitor Hs-27 and the fluorophore fluorescein isocyanate (FITC) were provided by Dr. Timothy Haystead's laboratory in the department of Pharmacology and Cancer Biology at Duke University.

Surgeries were performed to implant dorsal skinfold window chambers (Figure 1) according to the sterile procedure detailed by Palmer and colleagues (2011). The mice (n=3) were anesthetized using intraperitoneal injections of 100 mg/kg ketamine and 10 mg/kg xylazine and implanted with titanium window chambers on their dorsal skin flap. The thin layer of skin inside the window chamber boundaries was removed and a serum-free suspension of approximately 10^6 MDA-MB-231 cells was injected just beneath the exposed skin tissue of mice. A glass coverslip was placed to cover the exposed tissue.

Tumors were allowed to grow for approximately 10 days prior to hyperspectral and fluorescence imaging.

Hyperspectral and fluorescence imaging of *in vivo* Hs-27 uptake

After 10 days of growth, imaging with Hs-27 was performed on mice using a Zeiss Axioskop 2 microscope provided by the Optical Imaging Facility at the Duke Cancer Institute.

A 2.5x objective was used for vascular and fluorescence imaging with a Zeiss FluorArc mercury lamp. The imaging platform and heating pad for the mouse were set-up according to guidelines by the facility. Mice were under anesthesia using vaporized isoflurane within the 1.5-2 setting and eye drops were applied. The glass coverslip in the window chambers were cleaned with ethanol and positioned under the objective using a ruler, screws, and tape. The Shortcut to DVC program was opened and under Show Hb Sat Raw Images, settings were configured to wavelengths of 520-620 nanometer (nm) in 10nm increments, integration time of 200 milliseconds, and gain of 20 decibels.

The microscope light switch was covered, the microscope lever was changed to "FITC" and the lights in the room were turned off. Three baseline images were then taken for background determination. Tail vein injections of Hs-27 were administered at a 20mg/kg dose and images were taken periodically: every ten seconds for the first five minutes, every thirty seconds for the next 10 minutes and every three minutes for the next 75 minutes. After the 90 minutes of imaging, dark, neutral density filter (ND = 2.5), and rhodamine calibrations were performed.

Fourteen days post window chamber implantation, the mice were euthanized as the windows could not be kept longer than approximately two weeks when either the tumor grew larger than the window or the window started deteriorating (Palmer et al., 2011).

Data Analysis

Images were analyzed using MATLAB (matrix laboratory) program and all statistical testing were performed using R (R Foundation). T-tests were used for experiments comparing only two groups. Analysis of variance (ANOVA) with Tukey post hoc testing to calculate p-values was used for experiments with three or more groups. 0.05 was used as the significance level for all statistical tests.

Results

In vitro uptake of Hs-27 in BT-474, MCF-7 and MDA-MB-231 cells

To determine whether Hs-27, a novel fluorescently-tethered heat-shock protein 90 (Hsp90) inhibitor was effective in targeting breast cancer cells, live-cell imaging was performed to visualize and measure uptake based on fluorescence level. BT-474 (Her2 overexpressing), MCF-7 (estrogen receptor positive (ER+) and progesterone receptor positive (PR+), and MDA-MB-231 (triple negative) breast cancer cells were used to determine the receptor breast cancer cell line subtypes Hs-27 bound to and the level of affinity of the binding. Images from confocal microscopy showed that there was indeed uptake of Hs-27, which appears green in the presence of nuclear Hoechst (blue) staining. Across the different cell lines, there were different intensities measured for the fluorescence of Hs-27. The mean fluorescence was calculated from three regions of interest from two separate imaging sessions, and all cell lines were normalized so that the control images

averaged to a value of 1. BT-474 had a mean fluorescence intensity around 0.25 while MCF-7 and MDA-MB-231 had mean fluorescence intensities around 0.15 with p-values less than 0.001.

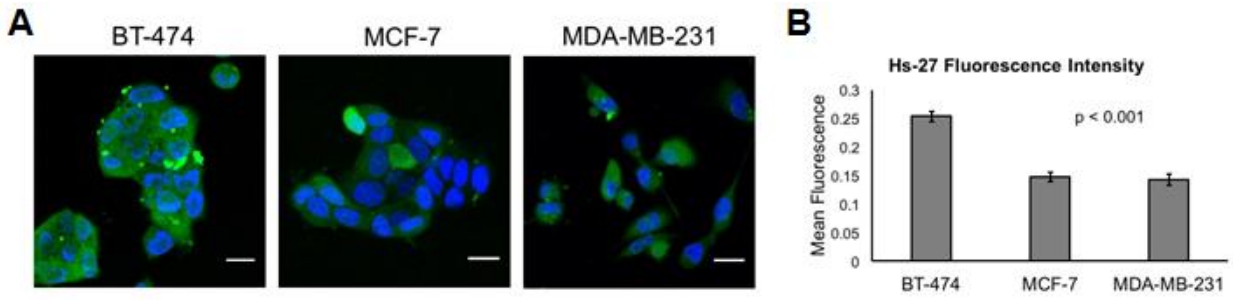

Figure 2: Hs-27 binds and shows different fluorescence signals in a variety of receptor subtypes. (A) BT-474 (Her2 overexpressing), MCF-7 (estrogen receptor positive (ER+) and progesterone receptor positive (PR+), and MDA-MB-231 (triple negative) breast cancer cells were grown for 24 hours before being treated for 15 minutes with 100uM Hs-27 (green). After washing the cells with PBS, Hoechst 33342 (blue) was added to stain nuclear DNA and confocal images were taken using a Zeiss 780 upright confocal microscope. Images from the confocal microscope show uptake of Hs-27(green) *in vitro* across all three cell lines. Scale bars are 20 um. (B) The plot shows the mean fluorescence from Hs-27 calculated from three images taken from two different plates of cells.

Hs-27 uptake in MDA-MB-231 *in vivo* dorsal window chamber model

Hyperspectral and fluorescence imaging depicts a higher overall fluorescence in tumor mice compared to non-tumor mice (Figure 3A). Kinetic curves of both tumor and normal mice show that there is an initial peak right after the tail-vein injections of Hs-27. This peak starts to diminish as the unbound Hs-27 clears out of interstitial space (Figure 3B). From calculating the ratio of fluorescence from Hs-27 in a tumor window to non-tumor window, the contrast in fluorescent peaks around 40-minutes post-injection and remains relatively constant out to 90 minutes (Figure 3C). For each mouse in the study, the cumulative distribution functions (CDFs) of Hs-27 fluorescence at 40 minutes ($Hs\text{-}27_{40}$) shows shifts to the right for the tumor bearing mice.

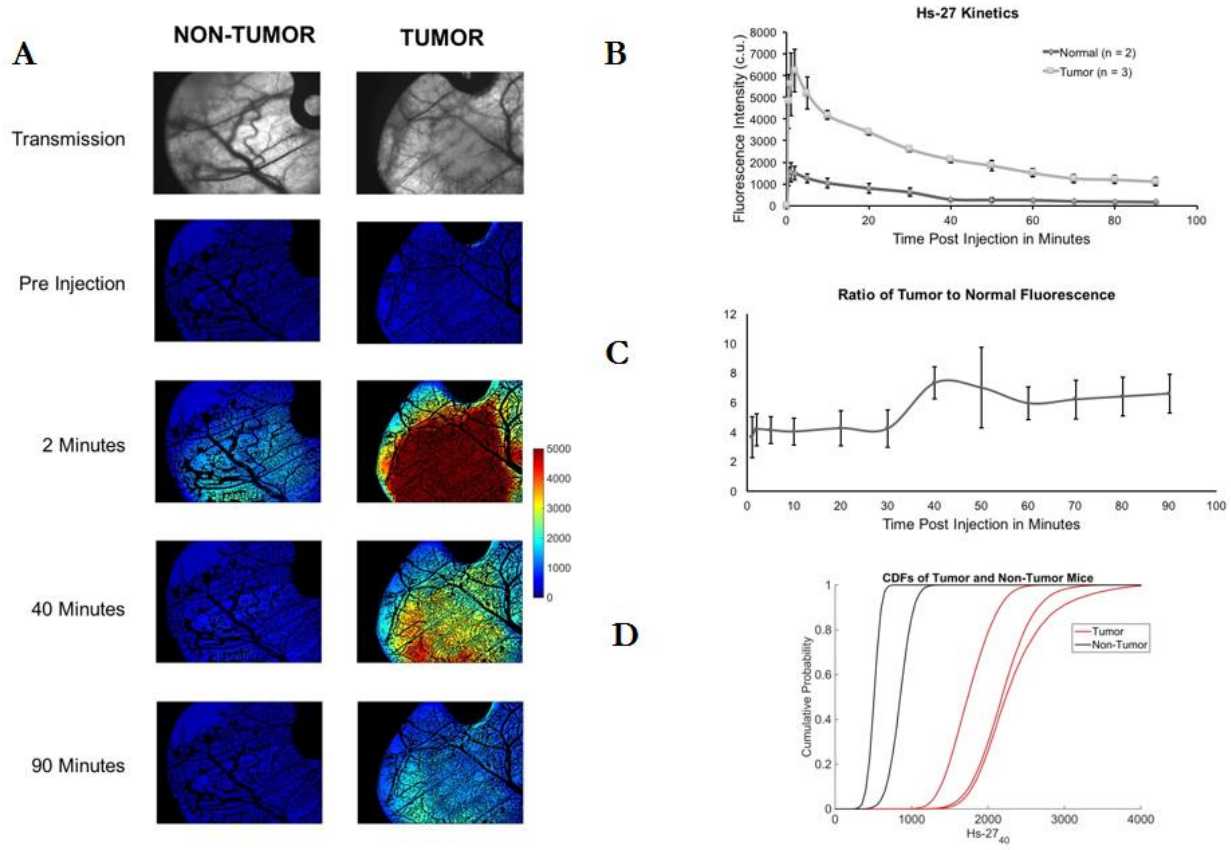

Figure 3: Hs-27 uptake is greater in MDA-MB-231 bearing mice than non-tumor mice. (A) Representative fluorescence images from tumor and non-tumor mice. (B) Hs-27 kinetic curves in both tumor and normal mice showing an initial peak after injection followed by a decrease in signal as unbound Hs-27 clears from the interstitial space. (C) Ratio of fluorescence from Hs-27 in a tumor window to non-tumor window reveals contrast peaks around 40-minutes post-injection and remains relatively constant out to 90 minutes. (D) Individual cumulative distribution functions (CDFs) of Hs-27 fluorescence at 40 minutes ($Hs\text{-}27_{40}$) for each mouse in the study. Tumor bearing mice have CDFs shifted to the right.

Discussion

Heat shock protein 90 (Hsp90) is a molecular chaperone widely distributed in all cells to assist in regulatory functions of proteins (Pearl & Prodromou, 2006). Since it is upregulated in cancer cells and correlated with a decreased survival rate in breast cancer, it has risen as an interesting anti-cancer target over the years (Moulick et al., 2011; Sahu et al., 2012). Hsp90 inhibitors such as the anti-biotic geldanamycin have anti-tumor activity,

which supports research efforts exploring this compound as a therapeutic (Miyata, 2005). However, there is still a need to produce safer and more efficacious treatment paradigms for cancers such as triple negative breast cancer (TNBC), the receptor subtype of focus in this study. Although TNBC is highly aggressive and difficult to treat due to its lack of susceptibility to hormone therapy, Hsp90 inhibitors may serve as effective chemotherapeutic agents. Hs-27 is a novel Hsp90 inhibitor which is advantageous because it has the potential to serve the role of a theranostic: a diagnostic and therapeutic tool. Overall, the purpose of this study was to determine the theranostic potential possessed by Hs27.

Preliminary experiments: Hs-27 uptake in cells

Initial experiments performed observed the specificity of Hs-27 binding to different subtypes of breast cancer cells. Confocal imaging (Figure 2) of Hs-27 treated BT-474 (Human epidermal growth factor 2 (HER2)) positive, MCF-7(estrogen receptor positive (ER+) and progesterone receptor positive (PR+)), and MDA-MB-231 (triple negative) cancer cells showed that there was indeed uptake of Hs-27. However, the uptake varied across all three cell lines, with BT-474 having the highest mean fluorescence, which could suggest that BT-474 may be the most likely to benefit from treatment with Hs-27

In another cell study, primarily performed by other members in the Ramanujam laboratory (See Appendix B), examining competitive binding of Hs-27 to Hs-10, which is the ligand component of Hs-27, we also observed variable binding of Hs-27 in the three breast cancer receptor subtypes. This in sum confirms that there is an interaction present with the overexpressed Hsp90 on the surface of the cancer cells.

In vitro therapy with Hs-27: Western blots

As a joint effort in the Hsp90 team in the Ramanujam lab, western blotting (See Appendix C) was performed to confirm that Hsp90 is expressed across all cell lines and is internalized in the cell at different rates, and to measure the expression of a number of proteins regulated by Hsp90, which are implicated in tumor proliferation. For BT-474, MCF-7 and MDA-MB-231, cells were treated at 10uM and 100uM concentrations at three time points of 12 hours, 24 hours and 48 hours to be able to find the optimal dose and time to decrease expression of these clients for each subtype. Clients stained for included Raf-1 kinase, Akt, and Hsp70, which are highly associated with tumor progression (Garcia-Echeverria and Sellers, 2008; Barrott et al., 2013). The blots showed varying results for each subtype of breast cancer. Akt and Raf-1 showed varying decreases, and as expected, Hsp70 levels increased as a compensatory mechanism of inhibiting Hsp90. Even with the rise of the co-chaperone Hsp70, the effect of Hs-27 was more prevalent in the overall treatment of the malignant cells. Overall, what can be gathered here is that Hs-27 is actively internalized after binding to Hsp90 on the cell surface, and that Hs-27 can decrease the expression of Hsp90 client proteins, which hints at the possibility of therapeutic use.

In vivo window chamber models and Hs-27 uptake

To determine whether similar outcomes would arise in animals, the study was translated to mice models in the form of patient-derived tumor xenografts (PDXs). Focusing solely on TNBC, window chamber tumors were implanted in dorsal skin flap window chamber models to allow for investigation of the kinetic profile of Hs-27 *in vivo.* Fluorescence images of tumor bearing and non-tumor bearing mice (Figure 3A) show that

there is higher uptake of Hs-27 overall in tumor-bearing mice, which suggests its specificity to malignant cells.

Additionally, kinetic curves (Figure 3B) show that both categories of mice possess similar profiles with an initial peak in fluorescence signals just after the tail vein injections and a waning of the signal overtime due to the clearance of unbound Hs-27 molecules. Comparing tumor to normal fluorescence during the 90 minute imaging interval revealed that the highest point of contrast was observed 40-minutes post injection, which is a helpful time point for further analysis (Figure 3C). At the 40 minute time point, individual cumulative distribution functions (CDFs) representing Hs-27 fluorescence for each mouse in the study showed that tumor bearing mice had CDFs shifted to the right. This rightward shift implies that there was higher fluorescence from the administration of Hs-27 in tumor bearing mice compared to non-tumor bearing mice, which confirms that Hs-27 has specificity for tumors *in vivo* (Figure 3D).

Conclusions and Future Directions

From both *in vitro* and *in vivo* studies, Hs-27 displayed its specificity for tumor cells through binding on the cell surface and tumor tissues, a step essential for its use as a diagnostic tool. Additionally, it has demonstrated therapeutic efficacy by its down-regulation of client proteins implicated in cancer. It would be worthwhile to continue to take advantage of the dual function of Hs-27 and investigate with PDXs to determine whether there are other facets of breast cancer that Hs-27 may thwart. For instance, cancer cells undergo the Warburg effect, where they prefer aerobic glycolysis, an inefficient source of glucose, even in aerobic conditions (Annibaldi & Widmann, 2010; Dang, 2012). Thus, it

would be valuable to determine whether and how Hs-27 affects this glycolytic ability (See Appendix D) and the implications in tumor viability. Furthermore, with continued exploration of Hs-27, an eventual goal is that this small molecule could be used to visualize residual disease after surgery and serve as a way to treat and monitor treatment responses.

Acknowledgments

I would like to recognize Brian Crouch for serving as my mentor and for his supervision throughout the project. I also want to extend a big thank you to Dr. Nimmi Ramanujam for giving me the opportunity to work and develop my interest in her laboratory. Additionally, I want to recognize Dr. Dave Sherwood, my faculty reader, for his guidance during my writing process. I want to thank all other members of the Ramanujam laboratory for their support in my research. Most importantly, special thanks to the Dean's Summer Research Fellowship and Goldman Sachs for research funding.

References

Annibaldi, A., Widmann, C. (2010). Glucose metabolism in cancer cells. Curr Opin Clin Nutr Metab Care, 13(4):466-70. doi: 10.1097/MCO.0b013e32833a5577.

Barrott, J. J., & Haystead, T. A. (2013). Hsp90, an unlikely ally in the war on cancer. *FEBS J, 280*(6), 1381-1396. doi:10.1111/febs.12147

Barrott, J. J., Hughes, P. F., Osada, T., Yang, X. Y., Hartman, Z. C., Loiselle, D. R., Spector, N.L., Neckers, L., Rajaram, N., Hu, F., Ramanujam, N., Vaidyanathan, G., Zalutsky, M.R., Lyerly, H.K., & Haystead, T. A. (2013). Optical and radioiodinated tethered Hsp90 inhibitors reveal selective internalization of ectopic Hsp90 in malignant breast tumor cells. *Chem Biol, 20*(9), 1187-1197. doi:10.1016/j.chembiol.2013.08.004

Becker, B., Multhoff, G., Farkas, B., Wild, P. J., Landthaler, M., Stolz, W., & Vogt, T. (2004). Induction of Hsp90 protein expression in malignant melanomas and melanoma metastases. *Exp Dermatol, 13*(1), 27-32. doi:10.1111/j.0906-6705.2004.00114.x

Callans, L. S., Naama, H., Khandelwal, M., Plotkin, R., & Jardines, L. (1995). Raf-1 protein expression in human breast cancer cells. *Ann Surg Oncol, 2*(1), 38-42.

Cheng, Q., Chang, J. T., Geradts, J., Neckers, L. M., Haystead, T., Spector, N. L., & Lyerly, H. K. (2012). Amplification and high-level expression of heat shock protein 90 marks aggressive phenotypes of human epidermal growth factor receptor 2 negative breast cancer. *Breast Cancer Res, 14*(2), R62. doi:10.1186/bcr3168

Chiosis, G., & Neckers, L. (2006). Tumor selectivity of Hsp90 inhibitors: the explanation remains elusive. *ACS Chem Biol, 1*(5), 279-284. doi:10.1021/cb600224w

Clarke, R., Tyson, J. J., & Dixon, J. M. (2015). Endocrine resistance in breast cancer - An overview and update. *Mol Cell Endocrinol, 418 Pt 3*, 220-234. doi:10.1016/j.mce.2015.09.035

Dang, C.V. (2012). Links between metabolism and cancer. Genes & Dev, 26: 877-890. doi:10.1101/gad.189365.112

Frees, A.E., Rajaram, N., McCachren, S.S. III, Fontanella, A.N., Dewhirst, M.W., Ramanujam, N. (2014). Delivery-Corrected Imaging of Fluorescently-Labeled Glucose Reveals Distinct Metabolic Phenotypes in Murine Breast Cancer. PLoS ONE 9(12): e115529. doi:10.1371/journal.pone.0115529

Garcia-Echeverria, C., Sellers, W.R. (2008).Drug discovery approaches targeting the PI3K/Akt pathway in cancer. Oncogene, 27, 5511–5526; doi:10.1038/onc.2008.246

Graner, M. W. (2015). HSP90 and Immune Modulation in Cancer *Advances in Cancer Research*: Academic Press.

Hudis, C.A., Gianni, L. (2011). Triple-Negative Breast Cancer: An Unmet Medical Need. *The Oncologist* vol. 16 Supplement 1 1-11

LoPiccolo, J., Blumenthal, G. M., Bernstein, W. B., & Dennis, P. A. (2008). Targeting the PI3K/Akt/mTOR pathway: effective combinations and clinical considerations. Drug Resistance Updates : Reviews and Commentaries in Antimicrobial and Anticancer Chemotherapy, 11(1-2), 32–50. http://doi.org/10.1016/j.drup.2007.11.003

Miyata, Y. (2005). Hsp90 inhibitor geldanamycin and its derivatives as novel cancer chemotherapeutic agents. *Curr Pharm Des, 11*(9), 1131-1138.

Mollapour, M., & Neckers, L. (2012). Post-translational modifications of Hsp90 and their contributions to chaperone regulation. *Biochim Biophys Acta, 1823*(3), 648-655. doi:10.1016/j.bbamcr.2011.07.018

Moser, C., Lang, S. A., & Stoeltzing, O. (2009). Heat-shock protein 90 (Hsp90) as a molecular target for therapy of gastrointestinal cancer. *Anticancer Res, 29*(6), 2031-2042. Retrieved from http://www.ncbi.nlm.nih.gov/pubmed/19528462

http://ar.iiarjournals.org/content/29/6/2031.full.pdf

Moulick, K., Ahn, J. H., Zong, H., Rodina, A., Cerchietti, L., Gomes DaGama, E. M., Caldas-Lopes, E., Beebe, K., Perna, F., Hatzi, K., Vu, L.P., Zhao, X., Zatorska, D., Taldone, T., Smith-Jones, P., Alpaugh, M., Gross, S.S., Pillarsetty, N., Ku, T., Lewis, J.S., Larson, S.M., Levine, R., Erdjument-Bromage, H., Guzman, M.L., Nimer, S.D., Melnick, A., Neckers, L., & Chiosis, G. (2011). Affinity-based proteomics reveal cancer-specific networks coordinated by Hsp90. *Nat Chem Biol, 7*(11), 818-826. doi:10.1038/nchembio.670

Nicholson, K. M., & Anderson, N. G. (2002). The protein kinase B/Akt signalling pathway in human malignancy. *Cell Signal, 14*(5), 381-395. Retrieved from http://www.ncbi.nlm.nih.gov/pubmed/11882383

http://ac.els-cdn.com/S0898656801002716/1-s2.0-S0898656801002716-main.pdf?_tid=7447b96c-cdc3-11e5-b2a8-00000aab0f02&acdnat=1454867685_27d645bd2a507c0ed7dd721c4e0f7b1c

Palmer, G.M., Fontanella, A.N., Shan, S. Hanna, G., Zhang, G., Fraser, C.L., & Dewhirst, M.W. (2011). *In vivo* optical molecular imaging and analysis in mice using dorsal window chamber models applied to hypoxia, vasculature and fluorescent reporters. *Nature Protocols* 6, 1355–1366

Parks, W. C., Wilson, C. L., & Lopez-Boado, Y. S. (2004). Matrix metalloproteinases as modulators of inflammation and innate immunity. *Nat Rev Immunol, 4*(8), 617-629. Retrieved from http://dx.doi.org/10.1038/nri1418

Pearl, L. H., & Prodromou, C. (2006). Structure and mechanism of the Hsp90 molecular chaperone machinery. *Annu Rev Biochem, 75*, 271-294. doi:10.1146/annurev.biochem.75.103004.142738

Pick, E., Kluger, Y., Giltnane, J. M., Moeder, C., Camp, R. L., Rimm, D. L., & Kluger, H. M. (2007). High HSP90 expression is associated with decreased survival in breast cancer. *Cancer Res, 67*(7), 2932-2937. doi:10.1158/0008-5472.can-06-4511

Prince, T., & Neckers, L. (2011). A network of its own: the unique interactome of the Hsp90 cochaperone, Sba1/p23. *Mol Cell, 43*(2), 159-160. doi:10.1016/j.molcel.2011.07.005

Proia, D. A., & Bates, R. C. (2014). Ganetespib and HSP90: translating preclinical hypotheses into clinical promise. *Cancer Res, 74*(5), 1294-1300. doi:10.1158/0008-5472.can-13-3263

Proia, D. A., Zhang, C., Sequeira, M., Jimenez, J. P., He, S., Spector, N., Shapiro, G.I., Tolaney, S., Nagai, M., Acquaviva, J., Smith, D.L., Sang, J., Bates, R.C., & El-Hariry, I. (2014). Preclinical activity profile and therapeutic efficacy of the HSP90 inhibitor ganetespib in triple-negative breast cancer. *Clin Cancer Res, 20*(2), 413-424. doi:10.1158/1078-0432.CCR-13-2166

Pulaski, B.A., Ostrand-Rosenberg, S. (2001). Mouse 4T1 breast tumor model. *Curr Protoc Immunol.* Chapter 20:Unit 20.2. doi: 10.1002/0471142735.im2002s39.

Roberts, P.J., Usary, J.E., Darr, D.B., Dillon, P.M., Pfefferle, A.D., Whittle, M.C., Duncan, J.S., Johnson, S.M, Combest, A.J., Jin, J., Zamboni, W.C., Johnson, G.L., Perou, C.M. & Sharpless, N.E. (2012). Combined PI3K/mTOR and MEK Inhibition Provides Broad

Antitumor Activity in Faithful Murine Cancer Models. Clin Cancer Res, 18; 5290. doi: 10.1158/1078-0432.CCR-12-0563

Sahu, D., Zhao, Z., Tsen, F., Cheng, C. F., Park, R., Situ, A. J., Dai, J., Eginli, A., Shams, S., Chen, M., Ulmer, T.S., Conti, P., Woodley, D.T., & Li, W. (2012). A potentially common peptide target in secreted heat shock protein-90alpha for hypoxia-inducible factor-1alpha-positive tumors. *Mol Biol Cell, 23*(4), 602-613. doi:10.1091/mbc.E11-06-0575

Samant, R. S., Clarke, P. A., & Workman, P. (2012). The expanding proteome of the molecular chaperone HSP90. *Cell Cycle, 11*(7), 1301-1308. doi:10.4161/cc.19722

Sawarkar, R., Sievers, C., & Paro, R. (2012). Hsp90 globally targets paused RNA polymerase to regulate gene expression in response to environmental stimuli. *Cell, 149*(4), 807-818. doi:10.1016/j.cell.2012.02.061

Sidera, K., & Patsavoudi, E. (2008). Extracellular HSP90: conquering the cell surface. *Cell Cycle, 7*(11), 1564-1568.

Siegel, R.L., Miller, K.D., Jemal A. (2015). Cancer statistics, 2015. *CA Cancer J Clin,* 65: 5–29. doi: 10.3322/caac.21254

Soga, S., Akinaga, S., & Shiotsu, Y. (2013). Hsp90 inhibitors as anti-cancer agents, from basic discoveries to clinical development. *Curr Pharm Des, 19*(3), 366-376.

Trepel, J., Mollapour, M., Giacconne, G., Neckers, L. (2010). Targeting the dynamic HSP90 complex in cancer. Nat Rev Cancer, 10(8): p. 537-49.

Trinklein, N. D., Chen, W. C., Kingston, R. E., & Myers, R. M. (2004). Transcriptional regulation and binding of heat shock factor 1 and heat shock factor 2 to 32 human heat shock genes during thermal stress and differentiation. *Cell Stress Chaperones, 9*(1), 21-28.

Whitesell, L., & Lindquist, S. L. (2005). HSP90 and the chaperoning of cancer. *Nat Rev Cancer, 5*(10), 761-772. doi:10.1038/nrc1716

Wiech, H., Buchner, J., Zimmermann, R., & Jakob, U. (1992). Hsp90 chaperones protein folding *in vitro*. *Nature, 358*(6382), 169-170. doi:10.1038/358169a0

Workman, P., Burrows, F., Neckers, L., & Rosen, N. (2007). Drugging the cancer chaperone HSP90: combinatorial therapeutic exploitation of oncogene addiction and tumor stress. *Ann N Y Acad Sci, 1113*, 202-216. doi:10.1196/annals.1391.012

Ying, W., Du, Z., Sun, L., Foley, K. P., Proia, D. A., Blackman, R. K., Zhou, D., Inoue, T., Tatsuta, N., Sang, J., Ye, S., Acquaviva, J., Ogawa, L.S., Wada, Y., Barsoum, J., & Koya, K. (2012). Ganetespib, a unique triazolone-containing Hsp90 inhibitor, exhibits potent antitumor activity and a superior safety profile for cancer therapy. *Mol Cancer Ther, 11*(2), 475-484. doi:10.1158/1535-7163.MCT-11-0755

Zagouri, F., Sergentanis, T. N., Nonni, A., Papadimitriou, C. A., Michalopoulos, N. V., Domeyer, P., Theodoropoulos, G., Lazaris, A., Patsouris, E., Zogafos, E., Pazaiti, A., & Zografos, G. C. (2010). Hsp90 in the continuum of breast ductal carcinogenesis: Evaluation in precursors, preinvasive and ductal carcinoma lesions. *BMC Cancer, 10*, 353. doi:10.1186/1471-2407-10-353

Zhou, D., Teofilovici, F., Liu, Y., Ye, J., Ying, W. W., Ogawa, L. S., Inoue, T., Lee, W., Adjiri-Awere, A., Kolodzieyski, L., Tatsuta, N., Wada, Y., &Sonderfan, A. J. (2012). Associating retinal drug exposure and retention with the ocular toxicity profiles of Hsp90 inhibitors. *Journal of Clinical Oncology, 30*(15). Retrieved from <Go to ISI>://WOS:000318009802478

Appendix A

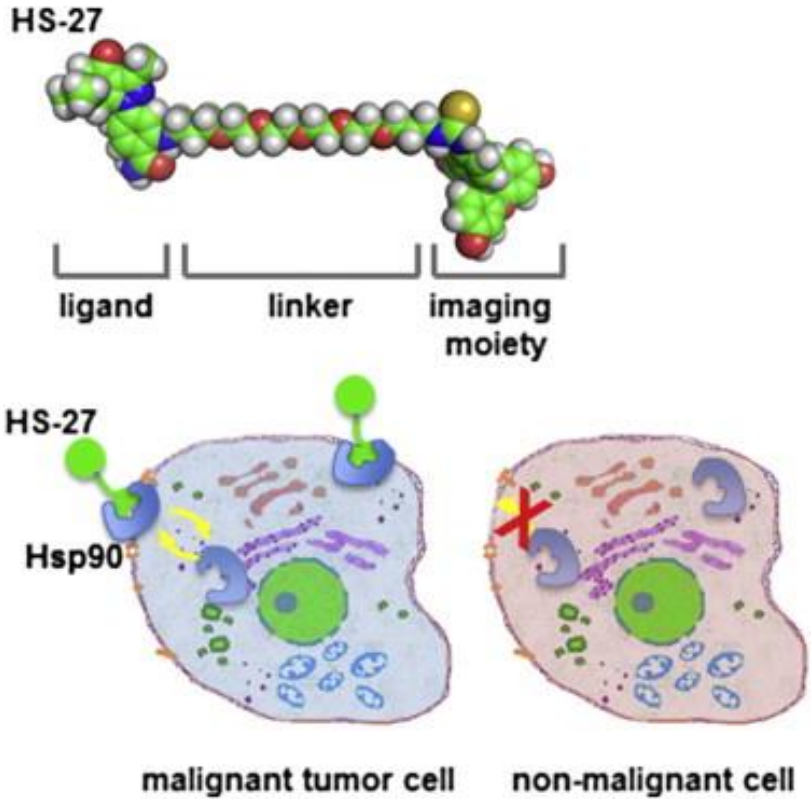

"Graphical Abstract." Retrieved from Barrott, J. J., Hughes, P. F., Osada, T., Yang, X. Y., Hartman, Z. C., Loiselle, D. R., Spector, N.L., Neckers, L., Rajaram, N., Hu, F., Ramanujam, N., Vaidyanathan, G., Zalutsky, M.R., Lyerly, H.K., & Haystead, T. A. (2013). Optical and radioiodinated tethered Hsp90 inhibitors reveal selective internalization of ectopic Hsp90 in malignant breast tumor cells. Chem Biol, 20(9), 1187-1197. doi:10.1016/j.chembiol.2013.08.004

Appendix B

Unpublished data from Brian Crouch, a Biomedical Engineering graduate student in the Ramanujam Laboratory

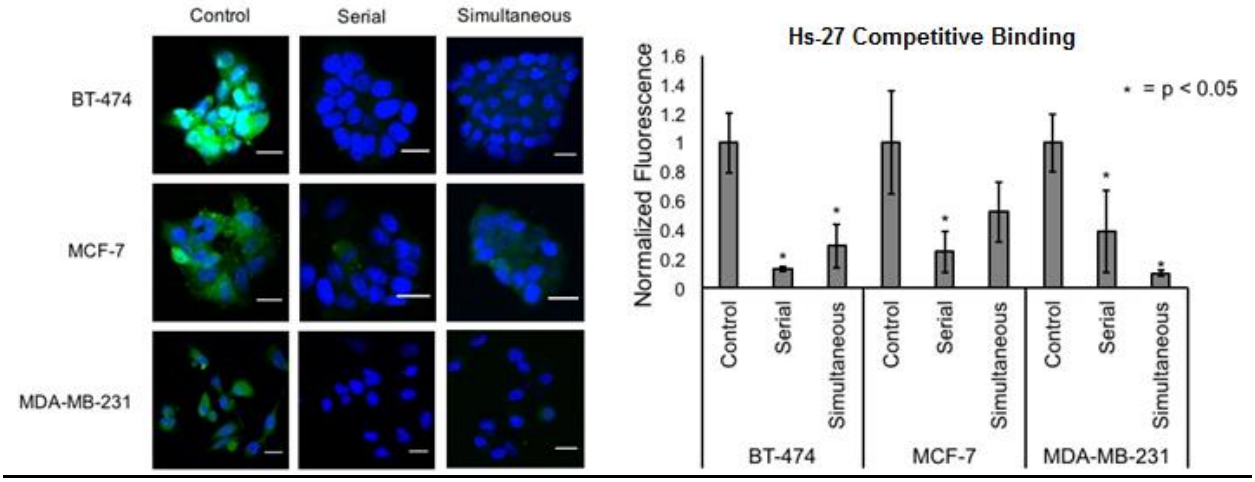

Figure 1: Hs-27 binds to a variety of cell lines *in vitro*, however, fluorescence is variable across different receptor subtypes. BT-474, MCF-7, and MDA-MB-231 cells were treated with Hs-27 only (control), serially with Hs-10 followed by Hs-27 (serial), or simultaneously with Hs-10 and Hs-27 (simultaneous) prior to imaging with a confocal microscope. Fluorescence was normalized so that the control images had a value of 1.

Appendix C

Unpublished data from Brian Crouch, a Biomedical Engineering graduate student in the Ramanujam Laboratory

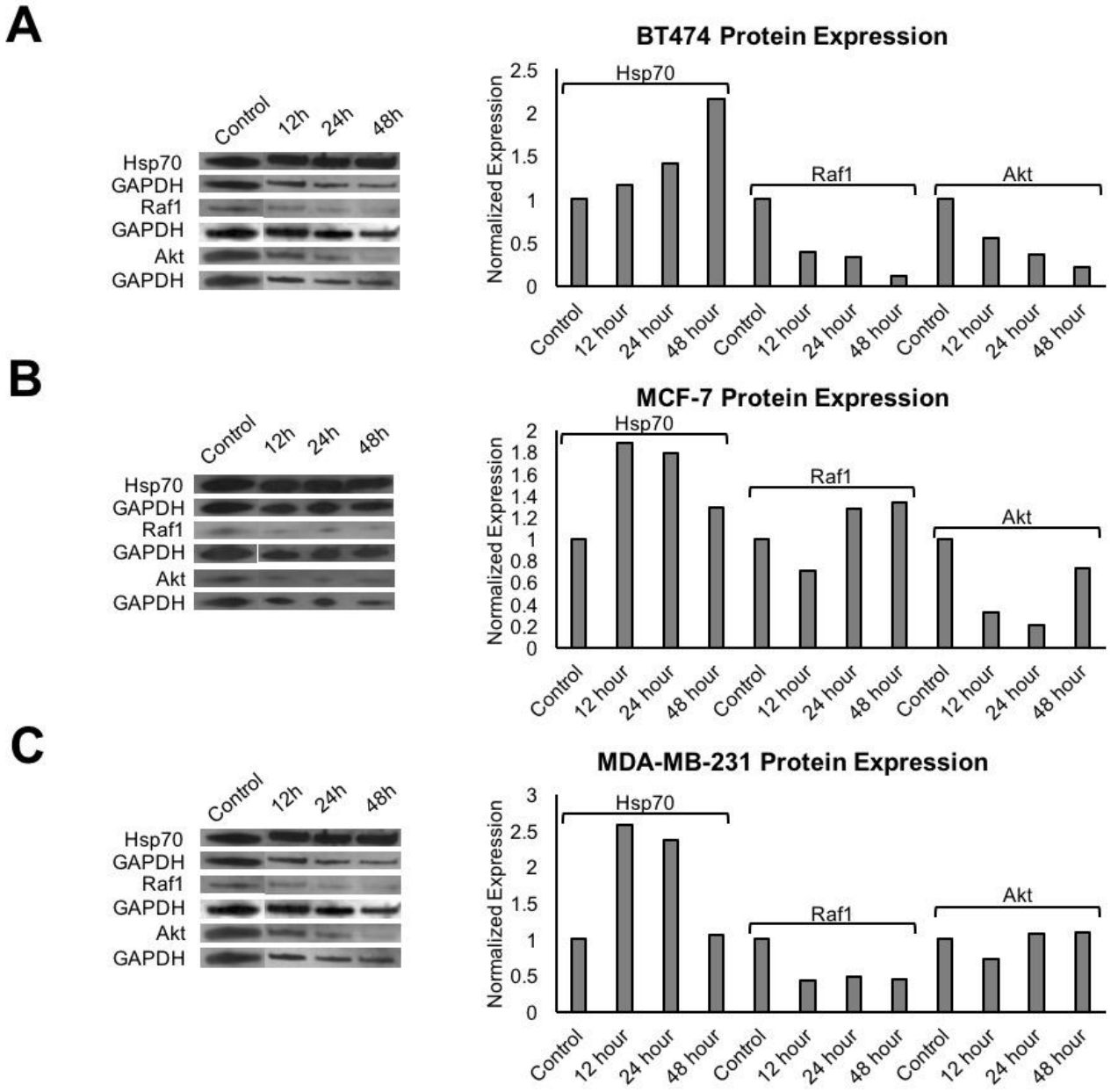

Figure 2: *In vitro* treatment with Hs-27 causes decreased Hsp90 client protein expression and changes in cellular metabolism. Western blotting was performed for Hsp70 (an Hsp90 co-chaperone protein), Raf1 (an Hsp90 client protein downstream of HER2 that can signal to increase cellular growth and proliferation), and Akt (an Hsp90 client protein involved in regulating glucose metabolism). (A) BT-474, (B) MCF-7, and (C) MDA-MB-231 cells were incubated for 12, 24, or 48 hours with 100uM Hs-27. Control cells

were incubated with DMSO vehicle. BT-474 cells showed increased Hsp70 and decreased Raf-1 and Akt at all time points relative to vehicle. Both MCF-7 and MDA-MB-231, however, show an initial increase in Hsp70 expression that returns to near baseline levels by 48 hours. MCF-7 cells show initial decreases in both Raf-1 and Akt that return to near baseline levels at later time points. MDA-MB-231 cells show a sustained decrease in Raf-1 expression from 12 to 48 hours. Akt, however, decreases initially and returns to near baseline levels.

Table 1: Summary of time to maximal and minimal expression for each cell-line/protein pair

	Hsp70 Maximum Expression	Raf-1 Minimum Expression	Akt Minimum Expression
BT-474	48 hours	48 hours	48 hours
MCF-7	12 hours	12 hours	24 hours
MDA-MB-231	12 hours	12 hours	12 hours

Appendix D

Experimental design for on-going Hs-27 studies

Implantation of MDA-MB-231 flank tumors

MDA-MB-231 cells were prepared in serum-free media at a concentration of approximately 5 x 10^6 cells per 100 μL. Mice (n=3) were placed under anesthesia using vaporized isoflurane within the 1.5-2 setting and flanks were cleaned using a gauze and ethanol. The suspension of cells were spun and 30 G x 1/2 in needles were used to inject 100 μL of the cell suspension subcutaneously into the flanks of 3 mice. Next, mice were weighed so that an initial weight could be kept for comparison because mice must to be euthanized if more than 15% of initial body weight is lost. Tumors were allowed to grow for 6 weeks with constant monitoring of growth by caliper measurements.

Diffuse Reflectance Spectroscopy of Hs-27 in Flank tumors

All spectroscopy was performed using instruments in the animal room of the Ramanujam laboratory. The lamp was turned on at least 30 minutes before use while the rest of the appliances were left on at all times. On the computer, the program "SynerJY" was used to collect measurements. The machine was calibrated at the beginning and the end of data collection for fluorescence using a white puck and for reflectance, which accounts for absorption and scattering in the tissue, using a gray puck with 20% reflectance. Calibration was performed by using the "Collect Experiment" set up tab, selecting "ok" and inputting either HSP_Single Fiber Probe REFL or FLUOR for their respective calibrations. Each mouse data collection was saved in the system following the format: Date_Hs-27_mouse number_cage card number. In this window, the Data Identifier followed the naming

convention “Puck Ref” or “Puck Fluor,” cycles were set to 1 because it was one measurement, and the command was run. To have an initial point of reference, baseline measurements were taken on the contralateral flanks under the Normal Fluorescence (NF) and Normal Reflectance(NR) settings and on the tumor flanks under the Tumor Fluorescence (TF) and Tumor Reflectance (TR) settings. Again, these were run at 1 cycle.

After baseline measurements were taken, tail vein injections of Hs-27 were administered and fluorescence measurements of tumor flanks were taken at 75 cycles with constant monitoring to ensure the probe did not move so that accurate fluorescence measurements could be collected. Lastly, a fluorescence measurement was taken of the contralateral (opposite) flank and the machine was calibrated as described earlier.

Hyperspectral and fluorescence imaging of in vivo 2-NBDG uptake

Window chamber surgeries were performed as detailed in the methods section. After 10 days of tumor growth, imaging was performed on a Zeiss Axioskop 2 microscope provided by the Optical Imaging Facility at the Duke Cancer Institute. The mice were imaged with 2-[N-(7-nitrobenz-2-oxa-1,3-diazol-4-yl) amino]-2-deoxy-d-glucose (2-NBDG), a fluorescent D-glucose derivative that can be used in optical imaging, as a marker to measure glucose uptake before and after treatment with Hs-10, the ligand from Hs-27 (Frees et al., 2014). The mice were imaged with 2-NBDG on the tenth day, treated with Hs-10 on the eleventh day, and imaged again with 2-NBDG on the twelfth day. The PI3 kinase/mTOR inhibitor BEZ-235 (Novartis) was used as a positive control.

A 2.5x objective was used for vascular and fluorescence imaging with a Zeiss FluorArc mercury lamp. The imaging platform and heating pad for the mouse were set-up according to guidelines by the facility. Mice were under anesthesia using vaporized isoflurane within the 1.5-2 setting and eye drops were applied. The glass coverslip in the window chambers were cleaned with ethanol and positioned under the objective using a ruler, screws, and tape. The Shortcut to DVC program was opened and under Show Hb Sat Raw Images, settings were configured to wavelengths of 520-620 nanometer (nm) in 10nm increments, integration time of 200 milliseconds, and gain of 20 decibels.

The microscope light switch was covered, the microscope lever was changed to "FITC" and the lights in the room were turned off. Three baseline images were then taken for background determination. Tail vein injections of the respective compound were administered and images were taken periodically: every ten seconds for the first five minutes, every thirty seconds for the next 10 minutes and every three minutes for the next 75 minutes. After the 90 minutes of imaging, dark, neutral density filter (ND = 2.5), and rhodamine calibrations were performed. Results from the FITC treatment were compared to results from Hs-27 treated MDA-MB-231 window chamber models in preliminary experiments.

Fourteen days post window chamber implantation, the mice were euthanized as the windows could not be kept longer than approximately two weeks when either the tumor grew larger than the window or the window started deteriorating (Palmer et al., 2011).